



Prepared jointly by
University of California
and
University of Chile

FAILURE ANALYSIS OF A REINFORCED CONCRETE FRAME STRUCTURE

TOMAS GUENDELMAN
GARY C. HART
RAUL HUSID

▶ FULL SCALE LABORATORY
EARTHQUAKE AND WIND ENGINEERING

UCLA - SCHOOL OF ENGINEERING AND APPLIED SCIENCE

An interpretation of this plastic seismic analysis in light of the observed structural failure is given in the text of the paper. Recommendations are made with respect to future design.

INTRODUCTION

On July 8, 1971 at 23:09 hours local Santiago, Chile time an earthquake of Richter magnitude 7.5 was detected at the University of California, Berkeley seismological station. The epicenter of this earthquake was located at latitude $32^{\circ} 45'$ South and longitude $71^{\circ} 58'$ West and at a depth of approximately 60 kilometers. The location of the epicenter is shown in Figure 1 and significant ground shaking was felt throughout central Chile.

A careful study of the damage experienced as a result of this South American earthquake is being made by the faculty of the University of Chile. (1)* The reader is referred to that report for a city-by-city description of damage. The authors have conducted a detailed study of the dramatic structural failure of a reinforced concrete frame building located in the city of Viña del Mar.

This paper describes the failure as well as a post-mortem analytical seismic analysis which was performed on the structure. First, a static dead load analysis of a typical interior frame was performed in order to estimate the frame's dead load bending moment diagram. Next, an eigenvalue analysis was performed on the same interior frame, assuming it to be linearly elastic, in order to determine its natural frequencies and normal mode shapes of vibration. Finally, a pseudo-dynamic failure analysis was carried out on the frame. In this latter analysis it was assumed that the seismic loading acted in a static manner and in proportion to the structure's generalized modal

* Numbers in paranthesis refer to References Listed at End of Paper.

displacement. This static loading was incrementally increased until structural collapse. Such a pseudodynamic analysis was necessary because no strong motion record existed at or near the structure's site.

This paper was encouraged and partially financed by the University of California-University of Chile Convenio Program. In August, 1971 as part of this program, Professors Gary C. Hart and C. Martin Duke of the University of California at Los Angeles, USA visited Chile and observed the damage experienced as a result of the July 8, 1971 earthquake.

DESCRIPTION OF THE STRUCTURE

The building under study is located in the city of Viña del Mar, see Figure 1, and approximately 50 kilometers from the epicenter of the July 8, 1971 earthquake. The city of Viña del Mar experienced significant ground shaking (peak acceleration estimated at approximately 20 percent gravity); and its Modified Mercalli Intensity was approximately VIII. Modern, reinforced concrete, high-rise buildings in the city experienced no major structural failure; however, most interior partitions had diagonal shear cracks. Also, significant damage was usually observed at the connection between two or more structural elements due to the differential movement. Major damage to exterior walls in the residential area and other smaller and older buildings was also observed.

The building discussed herein was constructed in 1946 and is one of two structurally identical reinforced concrete frame buildings. The structures are located within 20 meters of each other. One building experienced only minor visible damage during the earthquake; whereas the other building

suffered complete structural collapse. Figure 2 shows plan and elevation views of these buildings and Figure 3 shows photographs of the building which remained standing after the earthquake.

Certain particularities are evident in the building design. First, the concrete vaporization vents located at the apex of the rigid frame provide a large dead load and only nominal reinforcing. Second, the rigid frame reinforcement is continuous throughout the frame's beam-column region; and tension spalling of the concrete on the interior of this interface seems highly probable. Third, all reinforcing bars in this structure are underformed.

The 8 July earthquake caused one of the above noted buildings to completely collapse. Figures 4 and 5 show the post-earthquake condition of the building.

ANALYTICAL MODEL OF STRUCTURE

The reinforced concrete frame shown in Figure 2 was analytically modeled by the authors as a two-dimensional planar structure. We utilized the finite element method of analysis to discretize a typical interior frame into a finite number of beam elements, each beam element being allowed to have constant structural properties. It was assumed that the internal deformation pattern of each finite beam element is completely defined in terms of the two perpendicular translational and one rotational degree of freedom at its ends.

Figure 6 shows an elevation of the structural frame and the 22 beam finite elements comprising the analytical model. All finite beam elements except numbers 11 and 12 were assigned equal structural properties, see Table 1.

In all the analyses it was assumed that the base of the columns was rigid and that soil-structure interaction was not significant.

STATIC DEAD LOAD ANALYSIS

As a first step a static dead load analysis was performed on a typical interior frame. The tributary dead load acting on this frame was estimated to be 3.2 tons per horizontal meter. Figure 7 shows the frame's dead load bending moment diagram. Also shown in this figure is the plastic moment capacity of each structural element.⁽²⁾ It is immediately apparent that the dead load structural moments never approach the structure's plastic moment capacity, and in fact, the dead load factor of structural safety was never less than 2.

MODAL CHARACTERISTICS OF THE STRUCTURE

The finite element model was then utilized to calculate the frame's natural periods and mode shapes of vibration. A stiffness matrix condensation procedure was used to reduce the order of the system analyzed from 63 static to 26 dynamic degrees of freedom. In so doing it was assumed that the inertial effect of the loading associated with the axial deformation and joint rotation was negligible.

Table 2 lists the frame's first six natural periods of vibration and Figure 8 shows its first antisymmetrical and symmetric mode shapes.

PLASTIC FAILURE ANALYSIS

A step-by-step dynamic inelastic analysis of this structure was not felt to be warranted because there existed no time history of seismic ground

motion at or near the structure's site. Instead the authors decided to conduct a pseudo plastic dynamic analysis utilizing the structure's modal properties.

In the analysis performed, the static dead loads were first applied to the structure and the corresponding bending moments in all finite elements were calculated (Figure 7). Then, in addition to these dead loads a static loading equal in magnitude to a constant, α , times the frame's total tributary dead weight was added to the frame. In the first case studied, called Case A, the total dynamic load was distributed over the structure in proportion to the first antisymmetric modal displacements. The greatest modal displacement being set equal to unity. This case reflected a pseudo dynamic loading that was entirely lateral in direction and the constant α can be interpreted as the seismic lateral load coefficient. The second case studied, Case B, distributed the total pseudo dynamic load in proportion to the first symmetrical mode shape. This case resulted in a dynamic loading in the vertical direction and α can be interpreted as the seismic vertical load coefficient.

The analysis procedures followed in both cases were identical. First, the load coefficient, α , was increased in magnitude until a single plastic hinge was observed. Then the coefficient was increased even further in magnitude until a structural mechanism was formed and the frame collapsed.

Subjected to Case A type loading, the structure formed plastic hinges simultaneously at nodes 10 and 14 when $\alpha = 0.24$. The structure became a mechanism and hence collapsed at the slightly greater loading condition $\alpha = 0.25$. The mechanism of collapse was formed by the development of hinges at nodes 2, 10, 14, and 22. It is important that in this case where lateral

seismic loading was applied to the structure the increment of load necessary to go from first hinge to collapse was only one percent of the structure's weight.

The plastic response of the structure under vertical loading was studied in Case B. Here it was found that hinges were first formed at nodes 11 and 13 when $\alpha = 0.15$. Note that this seismic coefficient is significantly less than that of Case A. However, in Case B it was found that not until $\alpha = 0.52$ did a structural mechanism exist by virtue of hinges forming at nodes 2, 6, 11, 13, 18, and 22. A sketch of this failure mechanism under both of these loading cases is shown in Figure 10.

SUMMARY AND CONCLUSIONS

The performance of the formulated analytical structural model and the actual building was quite similar. Structural collapse was predictable from the structural model and hinge locations as postulated from the plastic analysis corresponded to observed failure mechanism.

It appears that the structural failure was a combination of vertical seismic forces which caused the formation of the first structural hinge and horizontal seismic forces which actually caused structural collapse.

This study recommends that seismic codes consider an extension of their static load concepts to include a seismic analysis of the type performed here in. Such an analysis includes both vertical and lateral seismic forces and their influence upon structural behavior.

REFERENCES

1. Universidad de Chile, Facultad de Ciencias Físicas y Matemáticas.
"Informe Preliminar Sobre el Sismo del 8 de Julio de 1971" (1971).
2. ACI Special Publication No. 17 - Volume I.
"Ultimate Strength Design Handbook".

TABLE 1
PROPERTIES OF STRUCTURAL ELEMENTS

Member Number	Bending Modulus of Elasticity	Shear Modulus of Elasticity	Moment of Inertia	Cross Sectional Area	Shape Factor
1-10, 13-22	2.1×10^6	0.84×10^6	1.82×10^{-2}	.27	1.2
11-12	2.1×10^6	0.84×10^6	14.00×10^{-2}	.69	1.2

Units: Tons - Meters

TABLE 2
NATURAL PERIODS OF VIBRATION

Mode Number	Period (sec)	Mode Type
1	0.52	1st Anti-Symmetric
2	0.25	1st Symmetric
3	0.12	2nd Antisymmetric
4	0.08	2nd Symmetric
5	0.04	3rd Antisymmetric
6	0.03	3rd Symmetric

First and second mode shapes are shown in figures 8 and 9.

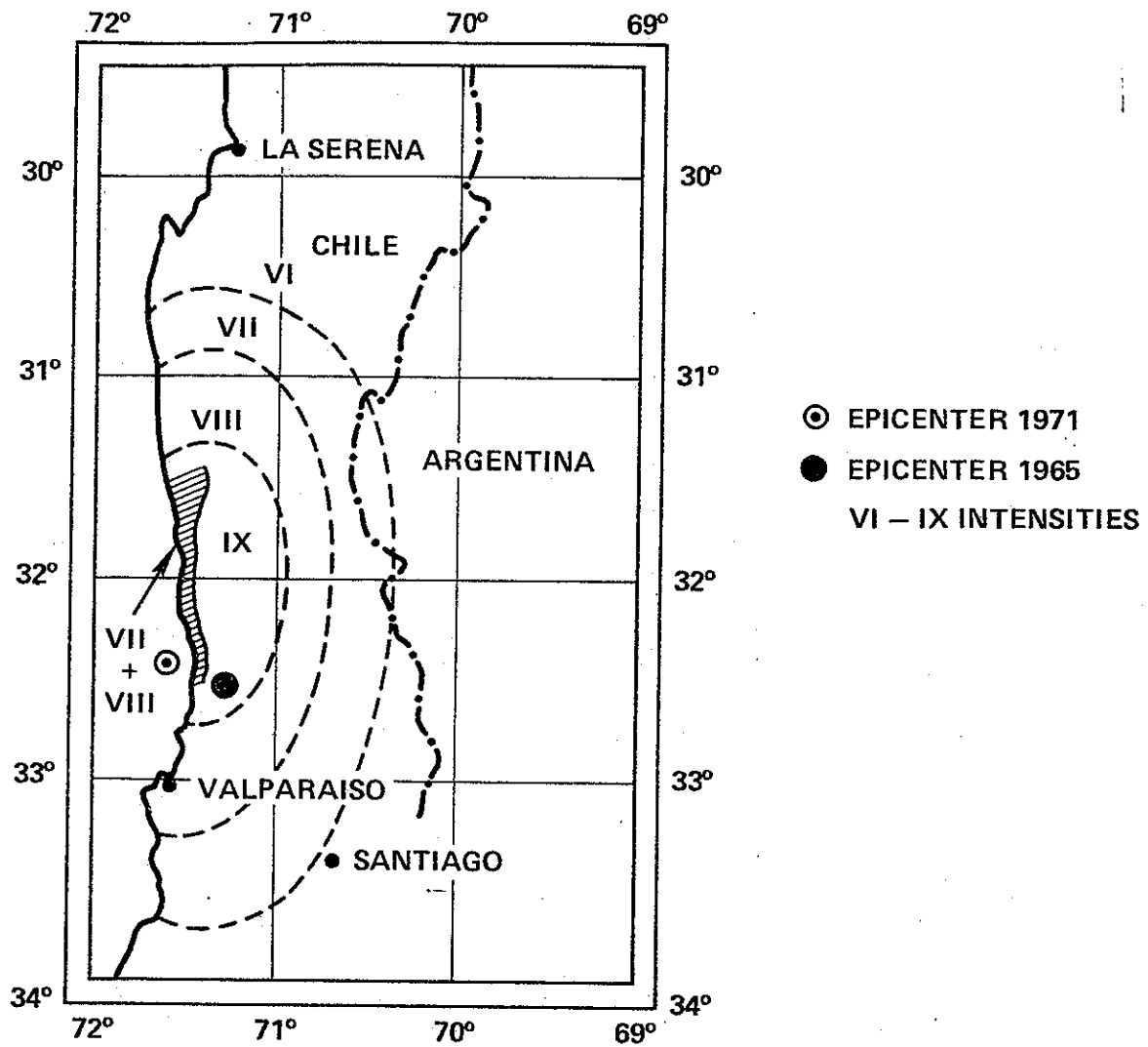


Figure 1. Location Map.

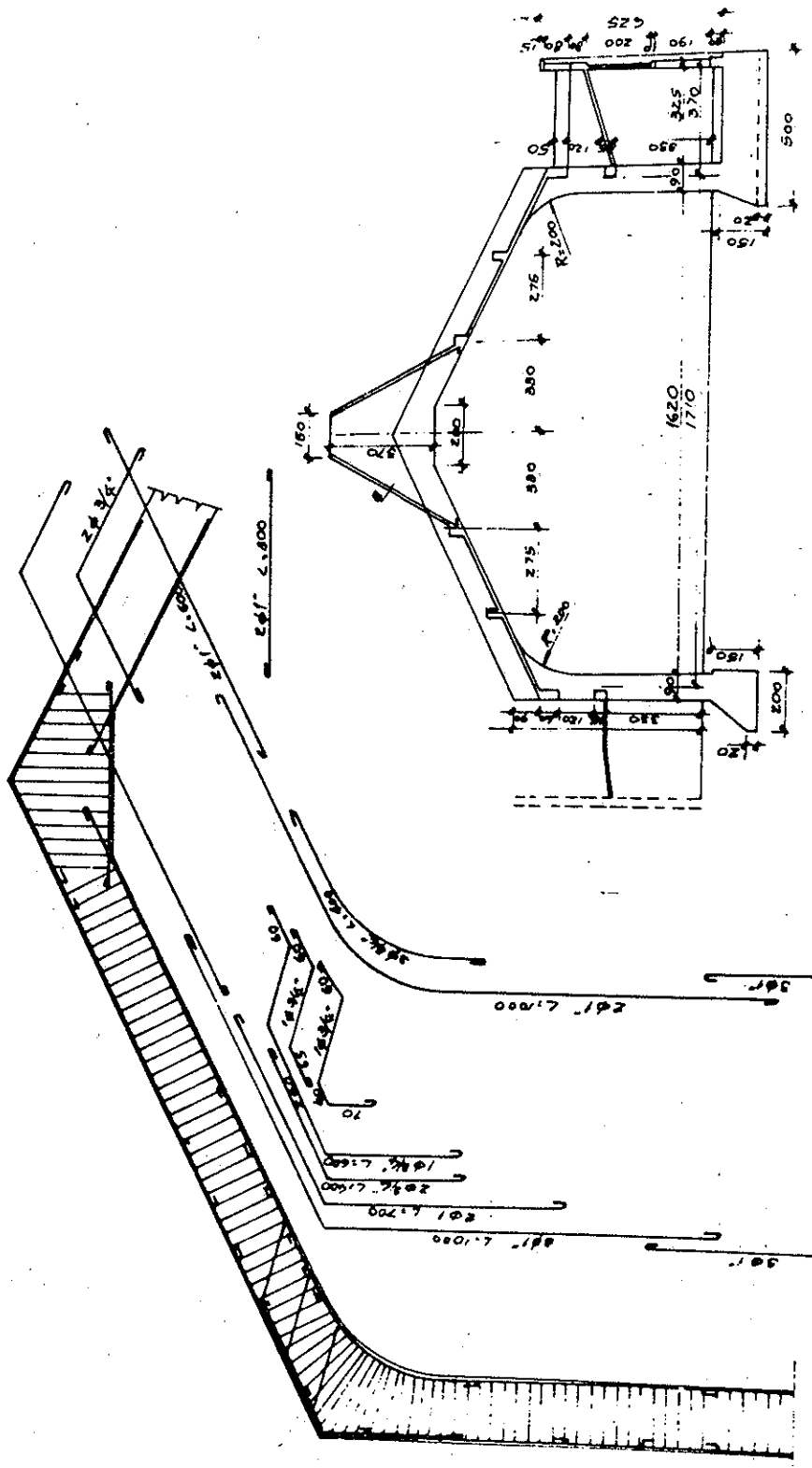


Figure 2b. Elevation of Building.

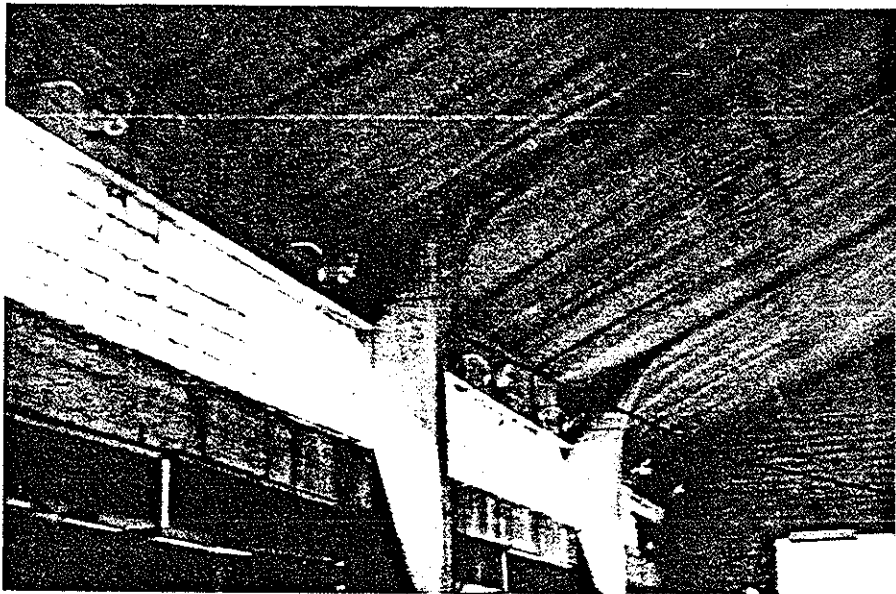
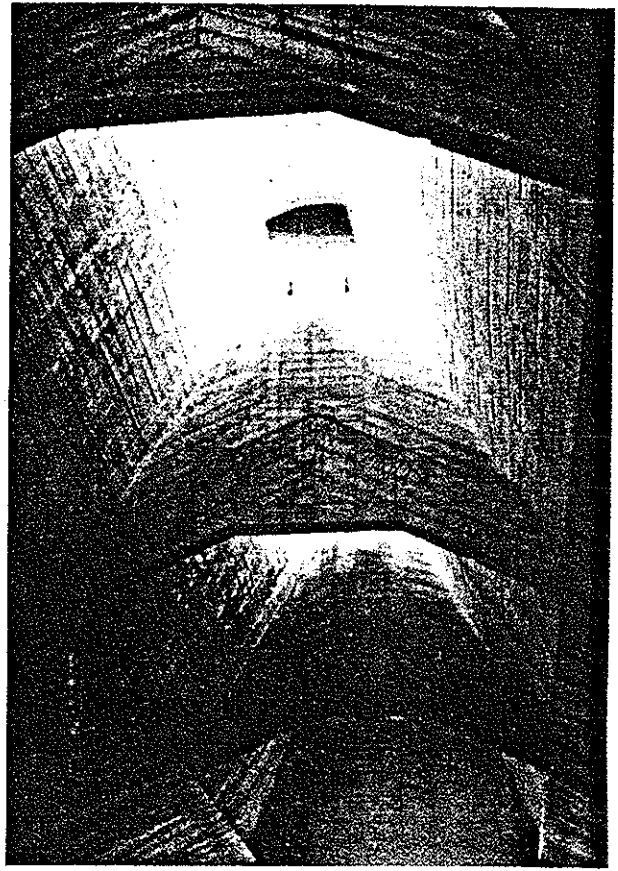


Figure 3. Photographs of Building: Pre-Earthquake

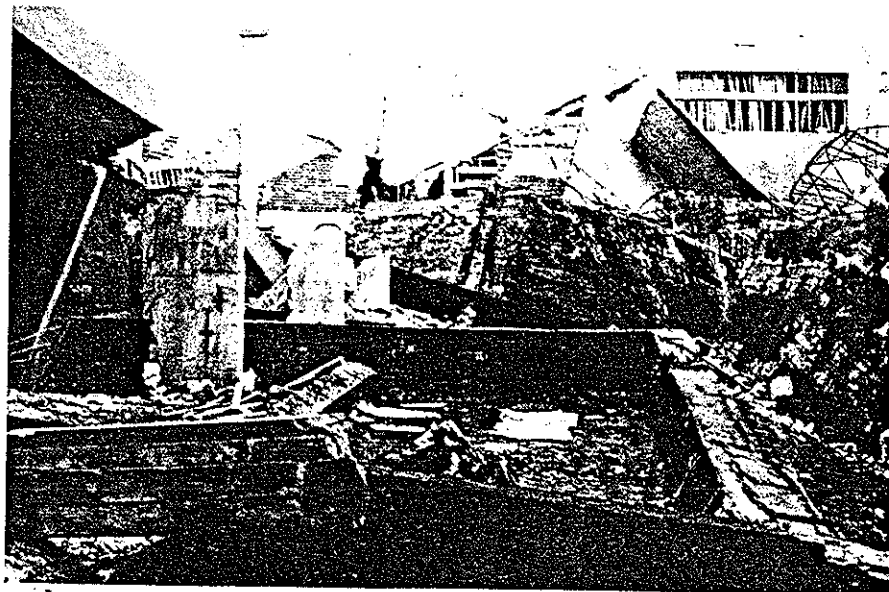
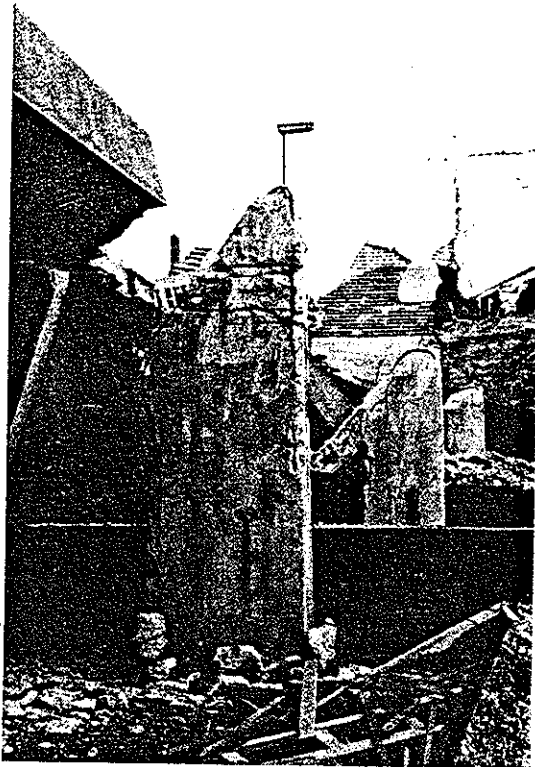


Figure 4. Photographs of Building: Post-Earthquake

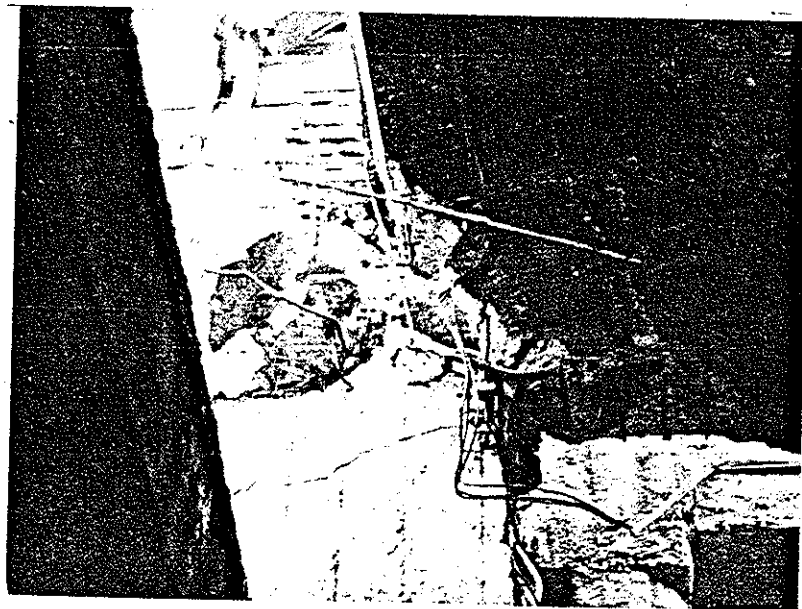


Figure 5. Photographs of Building: Post-Earthquake

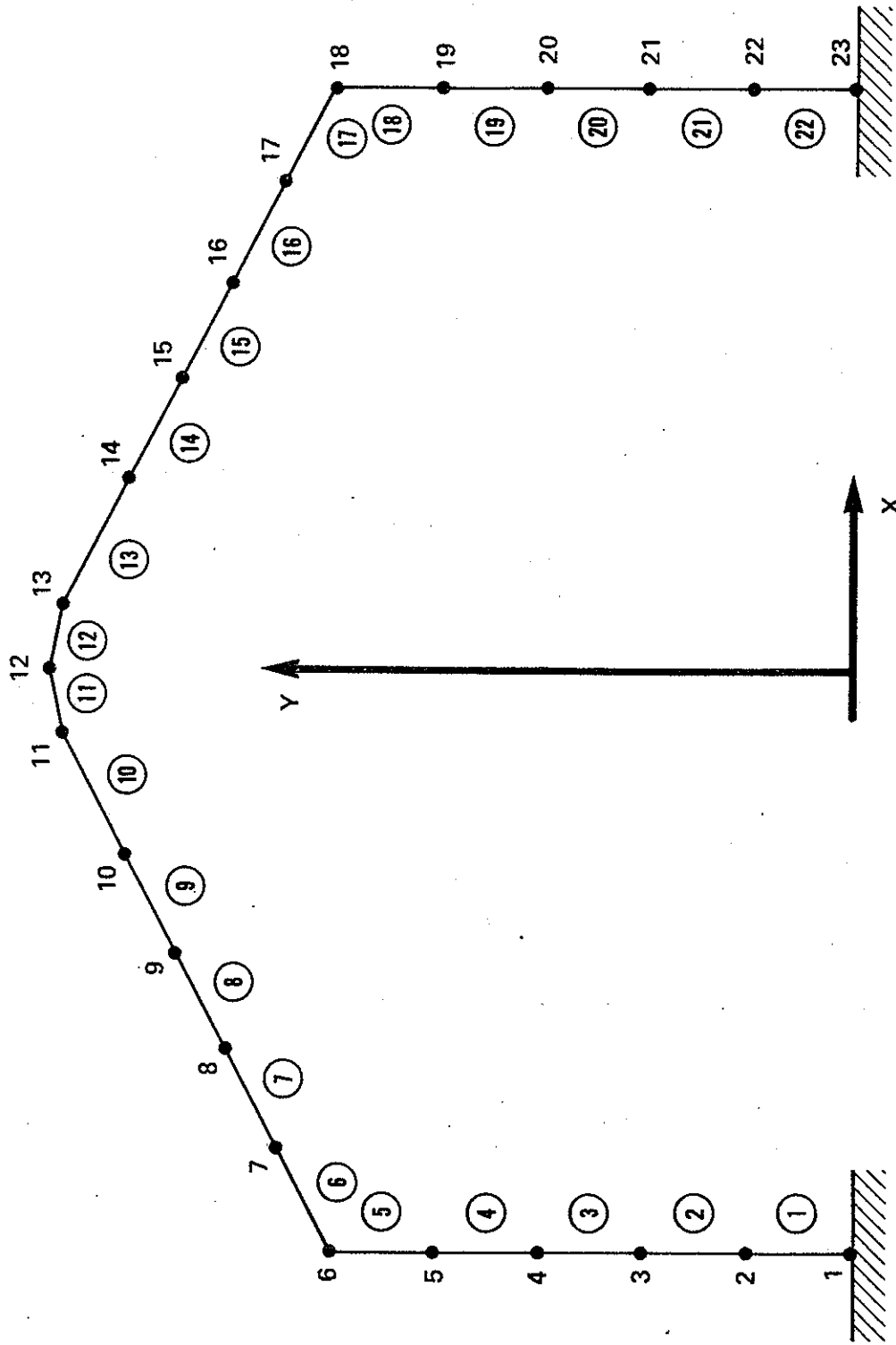


Figure 6. Structure Definition. Joint, Members and Coordinates.

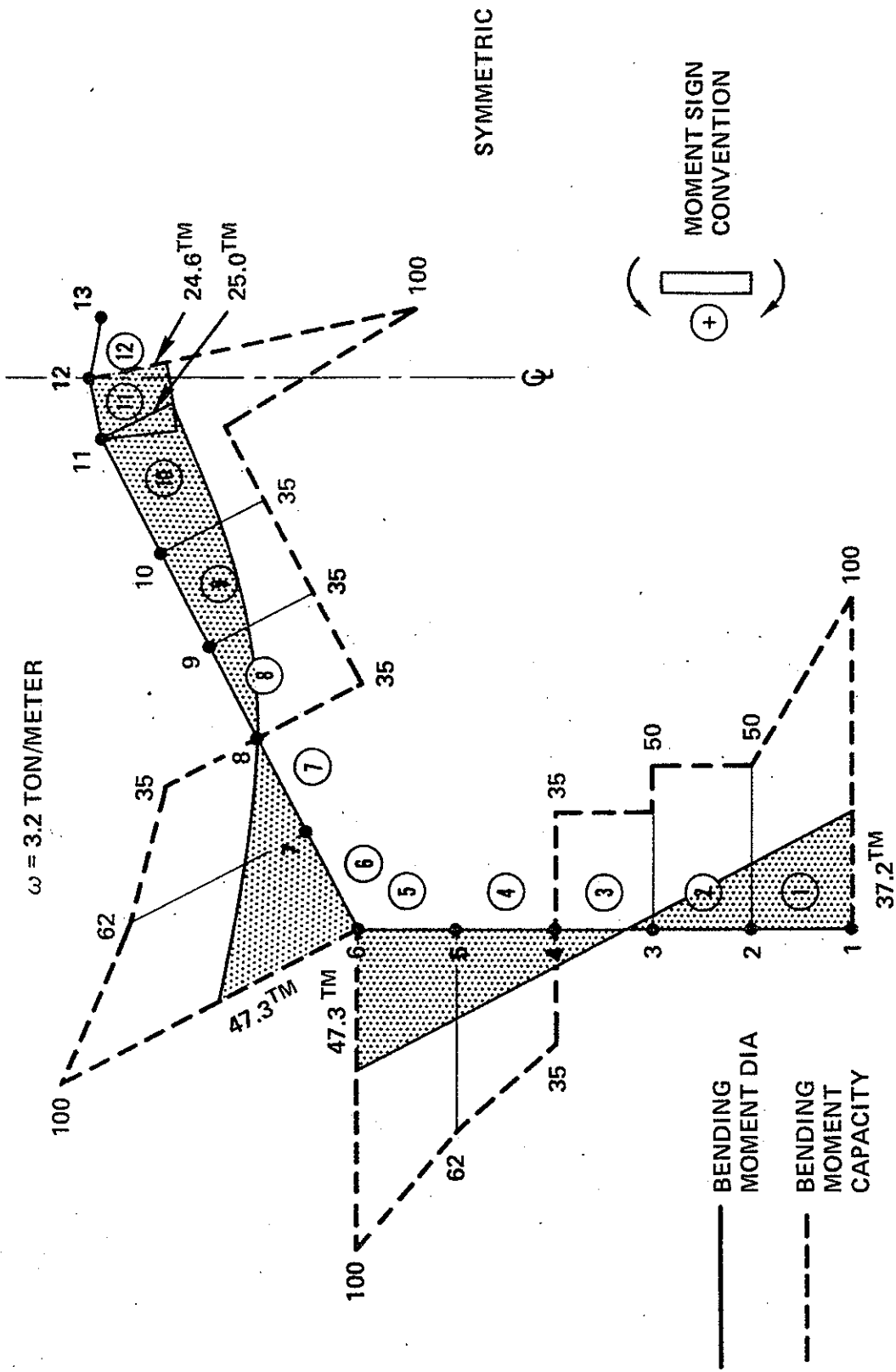
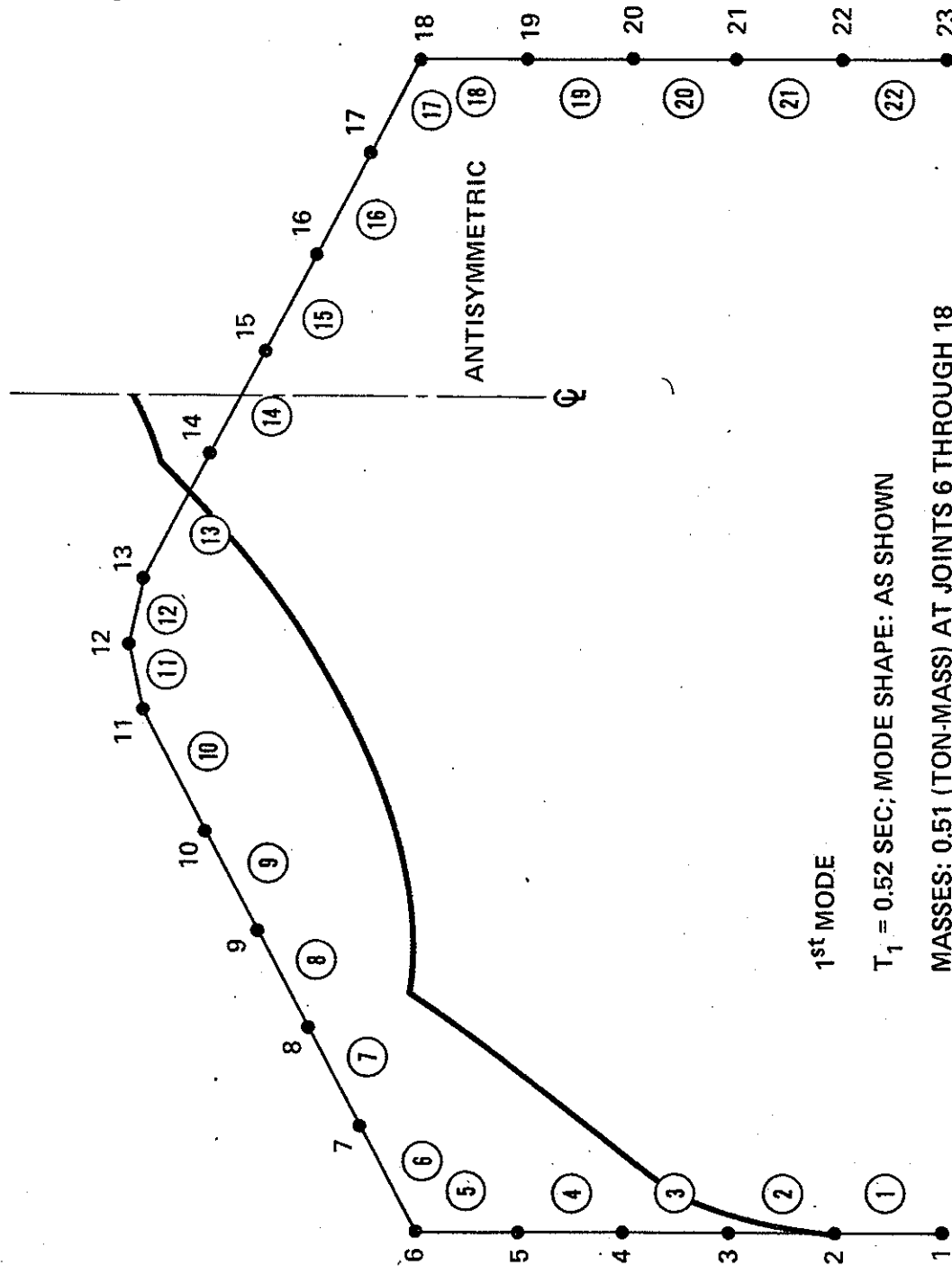


Figure 7. Bending Moment Diagram for Dead Load.



$T_1 = 0.52 \text{ SEC}$; MODE SHAPE: AS SHOWN

MASSES: 0.51 (TON-MASS) AT JOINTS 6 THROUGH 18

Figure 8. First Mode Shape.

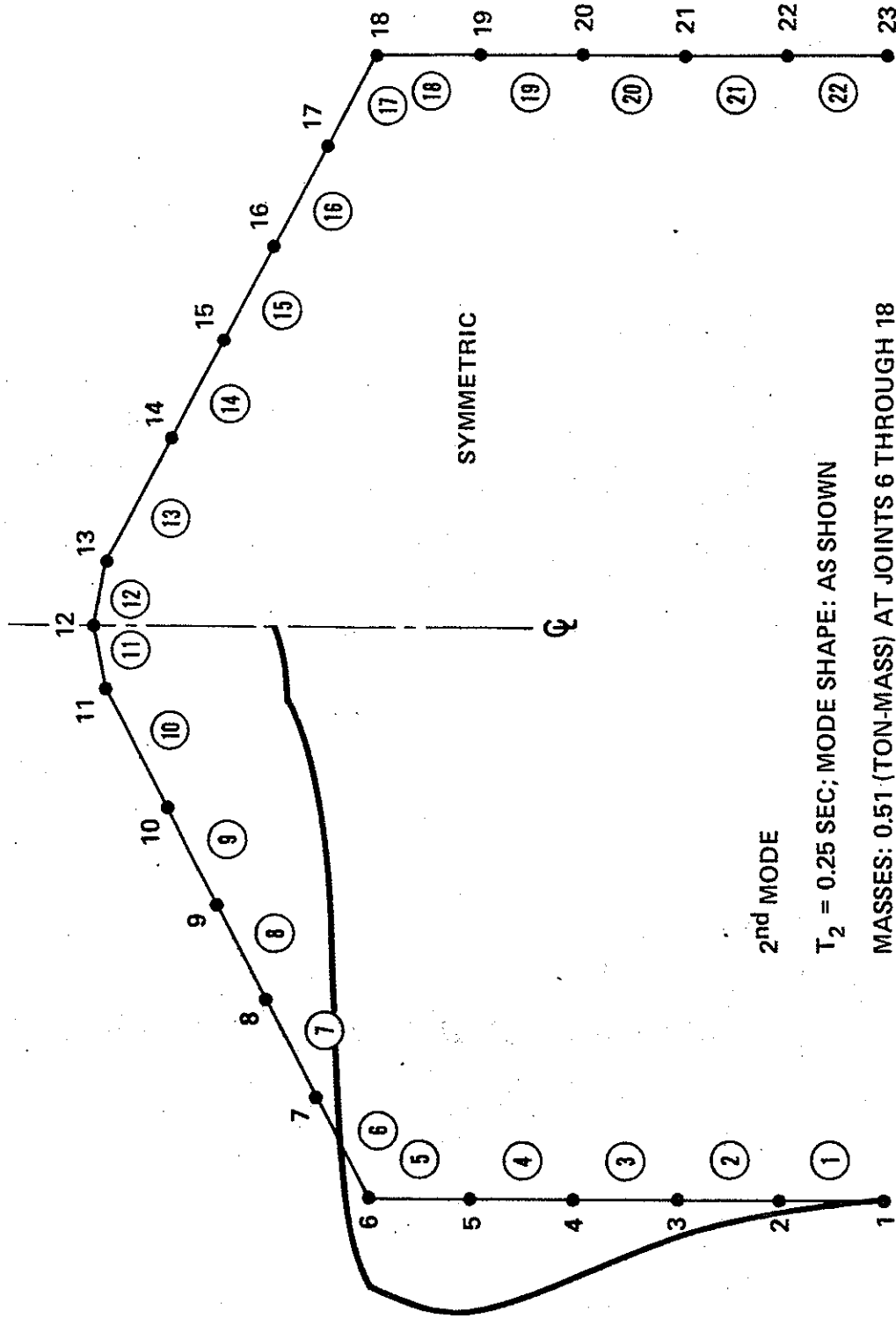


Figure 9. Second Mode Shape.

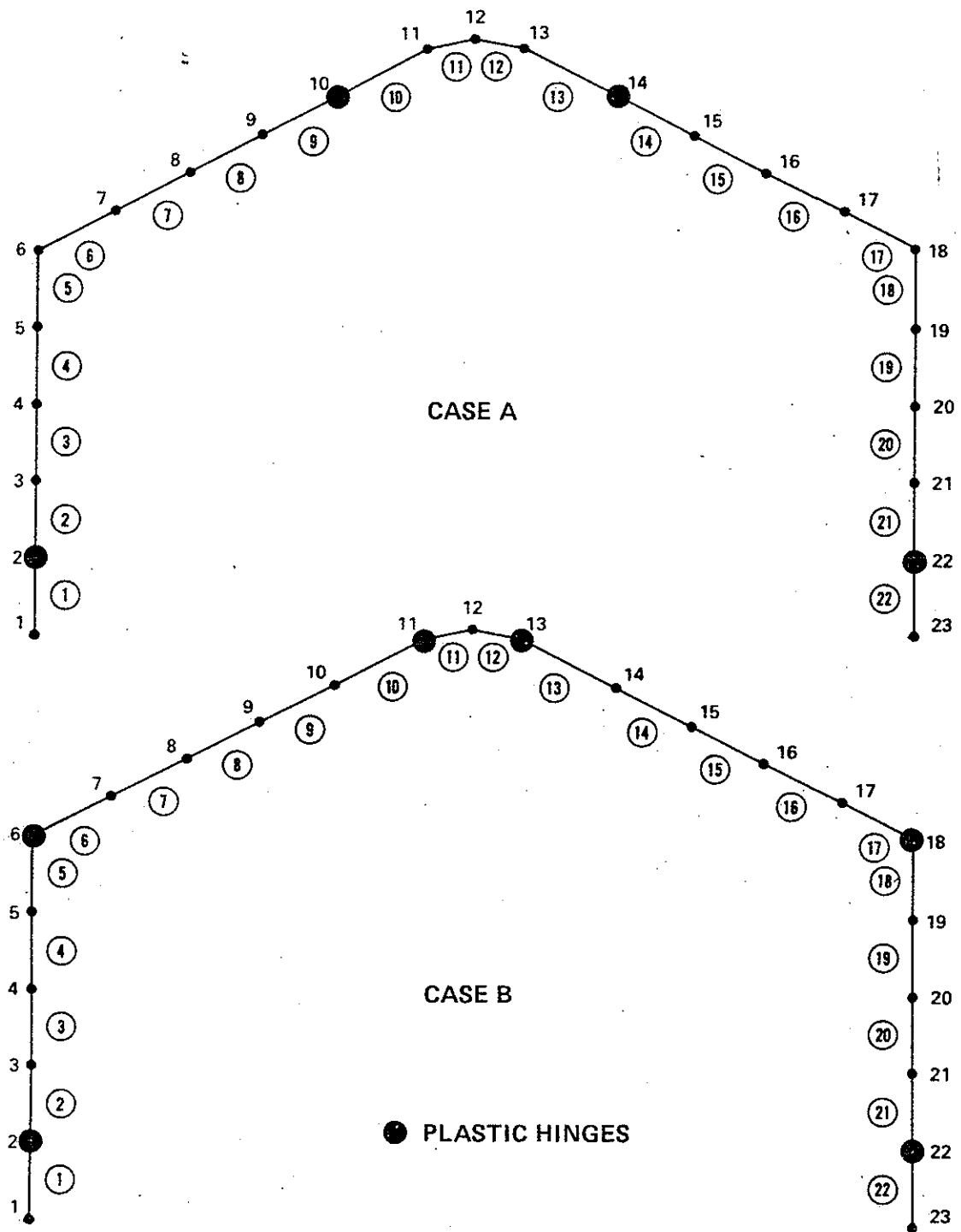


Figure 10. Failure Mechanisms.